HHS Public Access

Author manuscript

Nat Protoc. Author manuscript; available in PMC 2024 June 03.

Published in final edited form as:

Nat Protoc. 2022 June ; 17(6): 1468–1485. doi:10.1038/s41596-022-00689-4.

Subretinal injection in mice to study retinal physiology and disease

Peirong Huang[1,2,3], **Siddharth Narendran**[1,2,4], **Felipe Pereira**[1,2,5], **Shinichi Fukuda**[1,2,6], **Yosuke Nagasaka**[1,2], **Ivana Apicella**[1,2], **Praveen Yerramothu**[1,2], **Kenneth M. Marion**[7], **Xiaoyu Cai**[1,2], **Srinivas R. Sadda**[7,8], **Bradley D. Gelfand**[1,2,9], **Jayakrishna Ambati**[1,2,10,11,✉]

[1]Center for Advanced Vision Science, University of Virginia School of Medicine, Charlottesville, VA, USA.

[2]Department of Ophthalmology, University of Virginia School of Medicine, Charlottesville, VA, USA.

[3]Department of Ophthalmology, Shanghai General Hospital, Shanghai Jiao Tong University School of Medicine, Shanghai, China.

[4]Aravind Eye Care System, Madurai, India.

[5]Departamento de Oftalmologia e Ciências Visuais, Escola Paulista de Medicina, Universidade Federal de São Paulo, São Paulo, Brazil.

[6]Department of Ophthalmology, University of Tsukuba, Tsukuba, Japan.

[7]Doheny Eye Institute, Los Angeles, CA, USA.

[8]Department of Ophthalmology, David Geffen School of Medicine, University of California–Los Angeles, Los Angeles, CA, USA.

[9]Department of Biomedical Engineering, University of Virginia School of Medicine, Charlottesville, VA, USA.

[10]Department of Pathology, University of Virginia School of Medicine, Charlottesville, VA, USA.

✉**Correspondence and requests for materials** should be addressed to Jayakrishna Ambati. ja9qr@virginia.edu.

Author contributions

Conceptualization, P.H. and J.A.; investigation, P.H., F.P., S.N., Y.N. and S.F.; writing, P.H., F.P., S.N., K.M.M. and J.A. with assistance from I.A., P.Y., X.C., S.R.S. and B.D.G. All authors had the opportunity to discuss the results and comment on the manuscript.

Competing interests

J.A. is a cofounder of iVeena Holdings, iVeena Delivery Systems and Inflammasome Therapeutics, and has been a consultant for Allergan, Boehringer-Ingelheim, Immunovant, Olix Pharmaceuticals, Retinal Solutions and Saksin LifeSciences unrelated to this work. S.R.S. has been a consultant for 4DMT, Abbvie/Allergan, Apellis, Amgen, Centervue, Heidelberg, Iveric, Novartis, Optos, Oxurion, Regeneron and Roche/Genentech, received speaker fees from Novartis, Nidek, Carl Zeiss Meditec and Optos, and received research instruments from Carl Zeiss Meditec, Nidek, Topcon, Centervue, Optos and Heidelberg unrelated to this work; J.A. and B.D.G. are cofounders of DiceRx. J.A., S.N., I.A., F.P. and B.D.G. are named as inventors on patent applications filed by their university.

Extended data is available for this paper at https://doi.org/10.1038/s41596-022-00689-4.

Supplementary information The online version contains supplementary material available at https://doi.org/10.1038/s41596-022-00689-4.

[11]Department of Microbiology, Immunology, and Cancer Biology, University of Virginia School of Medicine, Charlottesville, VA, USA.

Abstract

Subretinal injection (SRI) is a widely used technique in retinal research and can be used to deliver nucleic acids, small molecules, macromolecules, viruses, cells or biomaterials such as nanobeads. Here we describe how to undertake SRI of mice. This protocol was adapted from a technique initially described for larger animals. Although SRI is a common procedure in eye research laboratories, there is no published guidance on the best practices for determining what constitutes a 'successful' SRI. Optimal injections are required for reproducibility of the procedure and, when carried out suboptimally, can lead to erroneous conclusions. To address this issue, we propose a standardized protocol for SRI with 'procedure success' defined by follow-up examination of the retina and the retinal pigmented epithelium rather than solely via intraoperative endpoints. This protocol takes 7–14 d to complete, depending on the reagent delivered. We have found, by instituting a standardized training program, that trained ophthalmologists achieve reliable proficiency in this technique after ~350 practice injections. This technique can be used to gain insights into retinal physiology and disease pathogenesis and to test the efficacy of experimental compounds in the retina or retinal pigmented epithelium.

Introduction

Subretinal injection (SRI) is used to access and deliver agents to the subretinal space. Clinically, it is a crucial step during vitrectomy surgery in the management of submacular hemorrhages[1] and retinal folds[2], and in delivering gene therapy to treat retinal dystrophies[3]. In retinal research, SRI is used mainly in rodent models for gene[4],[5] or cell[6] therapy research and to gain insights into retinal disease pathogenesis, especially in macular degeneration[7-17].

SRI in rodents was first described by Little et al., who transplanted human fetal retinal pigment epithelium into the subretinal space in a rat model of retinal degeneration[18]. Since then, SRI has been used extensively in retinal research not only for cell transplantation but also for gene therapy, understanding disease pathogenesis, identifying novel therapeutic targets, and testing the efficacy of potential therapeutics in several retinal diseases[7-15]. Our group discovered the key role of *Alu* RNA in the pathogenesis of age-related macular degeneration in 2011[7]. Using the SRI technique, we successfully established a model of atrophic (also known as dry) age-related macular degeneration in mice and identified multiple drug targets[7-15]. The SRI technique used in mice is more complex than in rats because of their smaller size. Here we provide details of how to inject mice, outlining the differences from the injection of rats, as applicable.

Applications of the SRI

In the past 10 years, the application of SRI in preclinical research and for clinical use has grown tremendously[19], as summarized in Fig. 1[8,11,13-15,20-35]. Although the subretinal route has been used extensively for administering adeno-associated virus (AAV) gene therapy vectors in mice, the use of this route to study phenotypic (degenerative) changes in the retinal pigmented epithelium (RPE) in mice has been reported by fewer groups,

with some researchers reporting difficulties in replicating this technique[21,36]. Proper execution of this technique is critical to obtaining valid insights into the molecular, cellular and anatomic effects of agent delivery. Also, the SRI technique is used to study neovascularization[21,22,37-42] and subretinal fibrosis[25,39,41].

Comparison with other methods

Three different techniques have been described to access the subretinal space in mice: the corneal approach, the transscleral approach and the pars plana approach (also named the limbal approach) (Fig. 2a-c, respectively). The transcorneal route, which consists of a needle passing the iris and lens through the pupil, is a common technique in studies where inducing a total retinal detachment may be desirable[43-45]. The transscleral posterior route, which is used to access the subretinal space without entering the vitreous cavity or penetrating the retina, is the mainstay procedure in newborn mice[46,47]. The pars plana approach, in which the needle is inserted via sclerotomy, permits direct visualization of the needle trajectory within the eye[37,48].

Here we describe the pars plana approach for SRI in mice. This approach was adapted from Bennet et al.[49], who initially described using it on larger animals. Direct visualization of the needle trajectory, the retinotomy site and the injection flow along with the absence of iatrogenic injury to the lens makes the pars plana approach advantageous compared with the other approaches. Our technique differs from a recent description of this technique in mice, wherein the authors define procedural success as the formation of a diffuse bullous retinal detachment[45]. However, it is already known that a high subretinal bleb will induce retinal degeneration in rabbits[50]. Moreover, a persistent separation between the neural retina and the underlying RPE can cause substantial variability of retinal or RPE injury in mice[51]. To test similar findings in mice, we repeated the procedure described in previous studies in which a large bleb is immediately evident after the successful injection of 0.6 μl phosphate-buffered saline (PBS) (Fig. 3c)[36,44]. This technique resulted in iatrogenic damage to the retina and the RPE, as evidenced by a large area of hypopigmentation in fundus photographs (Fig. 3g), subretinal vacuolization in image-guided spectral-domain optical coherent tomography (SD-OCT) images (Fig. 3h) and RPE degeneration in fluorescent micrographs of zonula occludens-1 (ZO-1)-stained RPE flat mounts (Fig. 3i), when compared with the representative images (Fig. 3d-f) from standard procedures (Fig. 3a, b) used in our protocol. On the basis of these results, we conclude that, although the initially described routes and endpoints for SRI might be sufficient to study cellular tropism or transduction efficacy of gene therapies, they are not ideal for studying the retinal phenotype or function.

Expertise needed to implement the protocol

The SRI technique requires a good working knowledge of the anatomy of the eye, preferably with prior microsurgical experience, appropriate equipment and dedicated practice. This considerable procedural requirement is consistent with our laboratory's experience of training two dozen personnel with prior ophthalmic surgical experience in this procedure over the past 20 years and has been formally studied in a recent study[52].

Limitations of the protocol

The lack of a histological macula (defined as the retinal region containing more than one row of retinal ganglion cells) in rodents is often cited as a limitation for studies on macular degeneration. However, the RPE in mice is not dissimilar to the human macular or perimacular RPE, which is nearly always the initial locus of RPE degeneration in macular degeneration. In addition, the phenotypic similarities of RPE degeneration in mice and human macular degeneration, as well as the availability of genetically modified strains, further support mice as an ideal species to study RPE degeneration. The other major technical concern is the extensive training and specialized equipment required for the proper adoption of this technique.

Experimental design

Overview of the Procedure—The general protocol for SRI requires reagent and animal preparation (Steps 1–7), SRI surgery (Steps 8–20), additional experimental treatment (Step 21) or use of transgenic mice, fundus photo examination (Steps 22–23), euthanasia and enucleation (Steps 24–25), sample collection (Steps 26–34) and confocal imaging (Steps 35–36; Fig. 4). After anesthesia and pupil dilatation, the reagent is delivered into the subretinal space by SRI. The phenotype of the RPE changes can be observed via fundus imaging, SD-OCT and ZO-1 staining of flat mount preparations at the suggested timepoints (Table 1). Other tissue samples can be collected for histological sectioning or extraction of RNA or protein according to specific experimental aims.

Controls—Negative and positive controls can be used in the training periods to improve surgical skills. Negative and positive controls for the technique could be selected from Table 1. This can help to distinguish whether the observed RPE degeneration is due to *Alu* RNA administration versus unsuccessful SRI.

Experimental animals—Adult mice aged 6–10 weeks are most suitable for the pars plana approach because their eye sizes are sufficiently large to facilitate surgical manipulation. Mice of older age and greater weight have relatively bigger eyeballs; therefore, this technique is expected to be even less difficult. For mice older than P10, transcorneal SRI can also be used[44]. For newborn mice whose eyes are even smaller, the transscleral posterior route is more suitable[46,47,53]. Thus the surgical approach should be tailored to the age and size of the mice required for experimental needs. Several mouse backgrounds with pigmented eyes are suitable for this model. Conversely, lack of RPE pigmentation renders the identification of the retinotomy and access to subretinal space challenging in B6 albino mice and other nonpigmented strains. No notable difference was observed between male and female mice in SRI. Male rats require more anesthetic supplementation because of greater lean body mass and more rapid metabolism[54]. In this protocol, we used adult C57BL/6J mice from 6 to 8 weeks of age, weighing 18–20 g for the SRI experiment (Supplementary Video 1). All procedures should be conducted in accordance with the Association for Research in Vision and Ophthalmology (ARVO) Statement for the Use of Animals in Ophthalmic and Vision Research (http://www.arvo.org/). Anesthesia and euthanasia must be performed in accordance with the institutional animal use committee guidelines.

Treatment procedure—The intravitreous route can be used to deliver treatment immediately after the SRI, using the same anesthesia procedure. The volume of intravitreous injection is usually 1 μl. The treatment can also be delivered by enteral or parenteral routes, with the total volume varying according to the animal weight.

Materials

Animals

Mice: we routinely use C57BL6J (6–8-week-old, The Jackson Laboratory) and other genetically modified mice according to experimental design **! CAUTION** All animal studies must conform to the appropriate governmental and institutional regulations. All animal experiments described in this protocol were approved by the University of Virginia Institutional Animal Care and Use Committees and were performed in accordance with the ARVO Statement for the Use of Animals in Ophthalmic and Visual Research.

Reagents

▲ **CRITICAL** Reagents and equipment identified are examples. Alternatives from other manufacturers can be used in substitution.

- 2,2,2,-tribromoethanol, 99% (Alfa Aesar, cat. no. 75-80-9)
- Alexa Fluor 594 (Invitrogen, cat. no. A32740; RRID: AB_2762824)
- Antifade mounting medium (Vectashield HardSet, cat. no. H-1400-10)
- Antifade mountant with DAPI (Invitrogen, cat. no. P36931)
- Anti-Cre rabbit polyclonal antibody (FITC), 1:1,000 (Novus Biologicals, cat. no. NB100-56133, RRID: AB_838060)
- Calcium and magnesium-free PBS (VWR Life Science, 10×, sterile, ultra-pure grade, cat. no. 97063-660)▲ **CRITICAL** Ultra-pure grade is important to avoid PBS-caused RPE degeneration.
- Carboxymethylcellulose 1% (Liquigel, Refresh)
- Electron microscopy sciences 32% paraformaldehyde solution (PFA; Fisher, cat. no. 50-980-495) **! CAUTION** PFA is a highly toxic irritant. Use personal protective equipment, protective gloves and eye or face protection before handling. Avoid breathing vapor. Wash hands thoroughly after handling.
- Erythromycin ophthalmic ointment, USP 0.5% (Bausch & Lomb, NDC 0574-4024-35)
- Ketamine hydrochloride (Fort Dodge Animal Health)
- Phenylephrine hydrochloride ophthalmic solution, USP 2.5% (Paragon Bio Teck, NDC 17478-201-15)
- Proparacaine hydrochloride ophthalmic solution, USP 0.5% (Bausch & Lomb, NDC 17478-201-15)

- Purified AAV stored at −80 °C (Vector Biolabs) **! CAUTION** AAVs are biohazardous materials and must be handled according to governmental and institutional regulations. Experiments involving AAVs require Biosafety Level 2 and Animal Biosafety Level 2 containment and safety practices as required by the US Centers for Disease Control and Prevention.
- Rabbit IgG (H+L) secondary antibody, 1:250 (Invitrogen, cat. no. A27034; RRID: AB_2536097)
- *tert*-Amyl alcohol (Emplura, cat. no. 8.06193.1000)
- Triton X-100 (Merck, cat. no. 1.08603.1000)
- Tropicamide ophthalmic solution, USP 1% (Akorn, NDC 17478-102-12)
- Xylazine (Phoenix Scientific)
- ZO-1 monoclonal antibody (ZO-1A12), Alexa Fluor 594, 1:100 (Fisher, cat. no. 339194; RRID: AB_2532188)

Equipment

- 0.22 μm polyethersulfone (PES) membrane filter unit (Millex-GP, cat. no. SLGP033RS)
- 10 ml syringe (BD, cat. no. 302995)
- 30 gauge (G) needle (BD, cat. no. 305128)
- Centrifuge (Eppendorf, cat. no. 5415D)
- Confocal microscope (A1R Nikon confocal microscope system, Nikon)
- Customized 37 G needle for mice (Ito)
- Customized 37 G needle for rats (Ito) ▲ **CRITICAL** It is crucial that the needles are airtight and have no dead space. Refer to the parameters and reference drawing of the needles in Extended Data Fig. 1.
- Deep freezer, −80 °C (Froilabo, cat. no. BM690)
- Dumont no. 7 curved forceps (Fine Science Tools, cat. no. 1129700)
- Fundus imaging camera (Topcon TRC-50IX) linked to a digital imaging system (Sony)
- Image-guided OCT (Phoenix Research Labs)
- Insulin syringes (BD, cat. no. 329461)
- Iris scissors, 4.5 inches (Graham-Field, cat. no. 2652)
- Microsyringe, 5 and 10 μl (Exmire MS-01, Ito) ▲ **CRITICAL** It is important that the microsyringes have no dead space, to achieve high reproducibility for the experiment ▲ **CRITICAL** 5 and 10 μl syringes are both suitable for the SRI injection. A 5 ▲l syringe is recommended for beginners as less fluid is injected with the same force applied on the plunger **! CAUTION** Avoid the use of highly

acidic substances as all parts of the syringe that make direct contact with the liquid are made of stainless steel (SUS316).

- Microscope slides (Fisherbrand, cat. no. 12-550-15)
- Optic lens (made from 200 ▲l tip; refer to Supplementary Video 2)
- PrecisionGlide Needle 30 G (BD, cat. no. 305106)
- Sterile alcohol prep pads (Fisher, cat. no. 22-363-750)
- T/Pump localized temperature therapy and Mul-T-pump local temperature therapy pad (e.g., Stryker)
- Vannas scissors curved (Storz, cat. no. E3387)
- Vortex (IKA minishaker MS2)

Reagent setup

Avertin stock solution—In a 20 ml glass vial, dissolve 10 g of 2,2,2,-tribromoethanol (99%) with 10 ml of tert-amyl alcohol. Store at room temperature (25 °C), avoiding light, for up to 6 months. For a working solution, add 1 ml stock solution to 39 ml PBS. Stir at 37 °C for 30 min before use. ▲ **CRITICAL** Avoid the formation of crystals in the final solution. Aliquot and store away from light at 4 °C. The working solution is stable for several months.

PFA solution, 2% (wt/vol)—Prepare fresh PFA solution by dissolving 3 ml 32% of PFA in 45 ml 1× PBS, and adjust the pH to 7.4. **! CAUTION** PFA is highly toxic and can cause irritation if exposed to skin, inhaled, or swallowed. A chemical fume hood and personal protective equipment including gloves and safety goggles are recommended when working with PFA.

Alu* RNA synthesis—Alu* RNAs can be synthesized as previously described[7-14,16]. Synthesize *Alu* RNA with an in vitro transcription kit (AmpliScribe T7-*Flash* Transcription Kit; Lucigen, ASF3507) from *Alu* expression plasmid with an adjacent T7 promoter. The sequence of the *Alu* RNA used in this protocol is GATCCTAATACGACTCACTATAGGGCCGGGCGCGGTGGCTCACGCCTGTAATCCCA GCACTTTGGGAGGCCGAGGCGGGCGGATCACAAGGTCAGGAGATCGAGACCATC CTGGCTAACACAGTGAAACCCCGTCTCTACTAAAAATACAAAAAATTAGCCGGGA GTGGTGTCGGGCGCCTGTAGTCCCAGCTACTCGTGAGGCTGAGGCAGGAGAATG GCGTGAACCCGGGAGGTGGAGCTTGCAGCGAGCCGAGATCGCGCCACTGCACTC CAGCCTGGGTGACAGAGCGAGACTCTGTCTCTTTAAAGGTAC. Treat the resulting *Alu* RNA with DNase, and purify (Nucleospin, RNA Clean-up, Macherey-Nagel, 740948.5). The integrity of the *Alu* RNA should be monitored by gel electrophoresis. The synthesized *Alu* RNA can be stored at −80 °C for 3 months.

Equipment setup

Housing and husbandry of experimental mice—House mice under a 12 h light cycle with water and chow provided ad libitum **! CAUTION** All experiments must be conducted

in compliance with the governmental and institutional guidelines for the care and use of animals within the research program.

Procedure

Reagent and syringe preparation ● Timing 30 min for 12 mice

▲ **CRITICAL** Reagent preparation should be carried out in a laminar flow hood equipped with UV light for sterilization. For RNA-related work, all work surfaces and equipment should be decontaminated with DNA and RNAZap before the experiment.

1. Prepare PBS by diluting 500 μl of 10× ultra-pure into 1× PBS using distilled water. Use a 0.22 μm PES membrane filter unit, to filter the 1× PBS solution. This filtered 1× PBS is ready to be injected into the animal or used for drug dilution, etc.

   ▲ **CRITICAL STEP** It is critical that an ultra-pure PBS is used to avoid RPE toxicity. Make fresh 1× PBS solution every time before the experiment.

2. Prepare the nucleic acids (RNA/DNA), AAV, RPE stressors or small molecules to be tested.

   ▲ **CRITICAL STEP** All reagents to be injected should be stored under reagent-specific conditions (temperature, RNase-free, etc.) before and during the procedure.

3. Store the syringes in ethanol. Before injection, attach the 37 G needle to the 5 μl syringe and wash with fresh ethanol three cycles, ddH_2O three cycles and 1× PBS three cycles, each cycle including ten times of aspiration and ejection of the wash buffer.

   ▲ **CRITICAL STEP** Proper sterilization of syringe and needle before the procedure is essential. After each injection, it is important to clean the needle with an alcohol pad and wait for it to dry before the next injection. The syringe should only be chemically sterilized, not by autoclaving. After the experiment, clean the syringe and needles in 1× PBS three cycles, ddH_2O three cycles and ethanol three cycles, each cycle including ten times of aspiration and ejection of the wash buffer. Then disassemble and store in ethanol.

Anesthesia and preparation of mice ● Timing 10 min per mouse

4 Set up the preparation area, surgical area and recovery area. Preparation area includes temperature therapy pad, drugs (tropicamide, proparacaine hydrochloride and carboxymethylcellulose 1%), 30 G needles, sterile alcohol prep pads and scissors. The surgical area is for the injection procedure. It includes a temperature therapy pad, head rest for mice, hand rest for the surgeon, needle washing buffer (ethanol, ddH_2O and PBS), syringe, optic lens, washing PBS, 30 G needle and tweezers. Refer to Supplementary Video 1 for details. The recovery area is for mice to awake from anesthesia on the temperature therapy pad after surgery.

▲ **CRITICAL STEP** SRI is a sterile technique. New surgeons should refer to the principles of rodent surgery[55].

5 Weigh the mice.

6 Dilate pupils with topical 1% tropicamide and 2.5% phenylephrine.

? TROUBLESHOOTING

7 Anesthetize mice. For mice, use intraperitoneal (i.p.) injection of 140–150 μl per 10 g of mouse body weight of Avertin. For both mice and rats, anesthesia can also be achieved by i.p. injection of 100 mg/kg ketamine hydrochloride and 10 mg/kg xylazine. To avoid cataract formation after anesthesia, keep the eye moistened by regular application of lubricant drops or gel. Turn on the temperature therapy pad, and set to 37 °C. After anesthesia, place the mice on the temperature therapy pad to avoid hypothermia. Trim the whiskers to avoid interference in the visual field of SRI procedures.

? TROUBLESHOOTING

Injection procedure ● Timing 1.5 h for 12 mice

8 Perform the SRI under direct visualization using a surgical microscope. Adjust the light intensity, focus and magnification to ensure proper visualization of the fundus.

▲ **CRITICAL STEP** A vitreoretinal surgical microscope (e.g., Leica F40) is highly recommended as it provides a higher-quality view of the fundus compared with a stereomicroscope (e.g., Nikon SMZ800N)

9 Fill the 5 μl syringe with 1–2 μl reagent. Prevent air bubbles in the solution.

▲ **CRITICAL STEP** We suggest using a custom 37 G needle with no dead space to ensure uniform volume delivery and prevent retinal degeneration by the procedure itself. Aspirating viscous samples by syringe can take more time (detailed parameters and design shown in Extended Data Fig. 1).

10 Elevate the head of the mouse by placing it on a head rest. The eye to be injected should be perpendicular to the microscope light.

11 Apply the proparacaine hydrochloride ophthalmic solution to the eye.

12 Under the surgical microscope, place an optic lens over the moistened cornea to allow visualization of the retina.

▲ **CRITICAL STEP** The diameter and width of the ring matter. A good ring includes holding the lubricant gel without leakage and a clear view of the fundus. For a 6–8-week-old mouse, a ring with a diameter of 3 mm and a height of 1.5 mm is recommended. Refer to Supplementary Video 2 for the detailed ring-making procedure.

13 Apply hydrogel to the optic lens.

? TROUBLESHOOTING

14 Adjust the microscope field, focus and light intensity until the fundus is visible.

▲ **CRITICAL STEP** The optic nerve should be visualized in the surgical field.

? TROUBLESHOOTING

15 Perform a sclerotomy 1 mm posterior to the limbus with a 30 G sterilized needle. Unlike Bennet et al[49]., we do not perform conjunctival peritomy because the mouse conjunctiva is extremely thin.

▲ **CRITICAL STEP** For consistency in the follow-up examination, we recommend that the sclerotomy and retinotomy be placed in the same quadrant among different mice. Moreover, the retinotomy is usually opposite to the sclerotomy site along the same axis. For example, if the sclerotomy is located on the nasal side of the sclera, the retinotomy site is better located in the temporal side of the optic nerve.

▲ **CRITICAL STEP** Do not insert the 30 G needle more than about halfway in. If it is inserted entirely, the hole will become too large and the intraocular pressure will quickly drop, which will easily cause a more extensive retinal detachment. Refer to Supplementary Video 1 for details.

▲ **CRITICAL STEP** Change the 30 G needle between mice to avoid infection.

! CAUTION Dispose of the 30 G needle after each procedure in an appropriate container.

? TROUBLESHOOTING

16 Using a 5 μl Ito syringe attached to a blunt 37 G Ito needle, introduce the needle at a 60° angle to avoid touching the lens (Supplementary Video 1). Introduce the needle under direct visualization until it touches the retina, ideally, 2–3 optic disc diameters from the optic disc.

▲ **CRITICAL STEP** It is essential the surgeon’s hand and the syringe are supported to prevent instability during the injection. If the needle is inserted too deep under the retina, it can easily cause subretinal hemorrhage. If the surgeon’s hand trembles, unnecessary force will be applied to the retina, causing a more extensive retinal detachment.

▲ **CRITICAL STEP** While introducing the needle inside the vitreous cavity, tilting the syringe to a closer angle (45°) makes it easier to reach the retina near the optic nerve.

▲ **CRITICAL STEP** Ensure the site of the retinotomy is away from the retinal vessels to avoid retinal/vitreous hemorrhage.

17 Apply gentle pressure on the retina by pressing the plunger to induce a retinotomy and provide access to the subretinal space. After that, perform SRI by slow and intermittent delivery into the subretinal space (Supplementary Video 1).

▲ **CRITICAL STEP** The ideal depth of the retinotomy is visualized by a brownish pigmentation at the retinotomy site. This represents RPE pigmentary dispersion and indicates a successful full-thickness retinotomy. Red discoloration can mean inadvertent injury to the choroidal vessels, and the procedure has to be terminated.

▲ **CRITICAL STEP** We suggest a slow and intermittent delivery over 45–60 s to ensure proper distribution of the injected solution and prevent localized bullous retinal detachment, which can lead to iatrogenic retinal degeneration.

▲ **CRITICAL STEP** The amount of material injected into the subretinal space may vary but should not be more than 1 μl in mice and should cause only a small, flattened bubble in the retina, not a bullous retinal detachment. For a rat, the injection volume could be as large as 4 μl of PBS without inducing degenerative changes.

? TROUBLESHOOTING

18 Withdraw the needle slowly, and avoid touching the retina or lens.

▲ **CRITICAL STEP** Wipe the 37 G needle with sterile alcohol prep pads between different mice to avoid infection. Wait for the needle to dry before further steps.

▲ **CRITICAL STEP** Wash the needle with 1× PBS ten times when the different reagents are to be delivered.

19 Check the fundus after 2–3 min to ensure no bullous retinal detachment and to judge intraoperative success.

▲ **CRITICAL STEP** A diffuse bullous retinal detachment shown in a previous protocol[45] induces iatrogenic retinal degeneration (Fig. 3c, g-i) after nontoxic PBS SRI. We define a minimal flattened elevation of the retina as an intraoperative success (Fig. 3b, d-f). Keep animal manipulation to a minimum to avoid ocular hypotony and retinal detachment.

? TROUBLESHOOTING

20 While the animal recovers from anesthesia on a temperature therapy pad, apply the antibiotic ointment to the eye to prevent postoperative infection. Apply the ointment gently to the cornea without damaging the cornea or applying pressure to the eyeballs.

? TROUBLESHOOTING

Mouse treatment ● Timing <3 min per mouse, per treatment

21 Administer treatments via intravitreous (option A) or i.p. (option B) routes.

A. Intravitreous injections

▲ **CRITICAL** Intravitreous injections can be either delivered immediately after SRI (Step 19) or at a selected timepoint according to the experiment design.

i. Prepare 1 μl of the drug in another 37 G needle + 5 μl syringe.

ii. Advance the needle into the eye through the same punctured hole.

▲ **CRITICAL STEP** Be careful not to exert external pressure on the globe as this can lead to hypotonia and retinal detachment.

iii. Introduce the needle until the tip is close to the retina, and deliver the agent.

▲ **CRITICAL STEP** Wait for 20–30 s before removing the needle from the eye. This prevents the reflux of the intravitreous injection.

? TROUBLESHOOTING

B. I.p. injection

▲ **CRITICAL** I.p. injection can be delivered at any time according to the experiment design.

i. Perform i.p. injection according to experiment design.

! CAUTION This step must conform to the appropriate governmental and institutional regulations. It should be performed in accordance with the ARVO Statement for the Use of Animals in Ophthalmic and Visual Research.

Fundus imaging ● Timing 30 min for 12 mice

▲ **CRITICAL** Fundus imaging can be undertaken at any time after injection in accordance with the particular aims of the study. The recommended observation timepoints for the positive and negative controls are listed in Table 1.

22 Dilate mouse eyes with topical 1% tropicamide and 2.5% phenylephrine.

23 Take fundus photos of mice (Table 1). Anesthesia is not necessary while using the fundus imaging camera (Topcon). A standard fundus photo of an eye should include the optic nerve, injection site and surrounding injected area (Fig. 5a,b).

Mouse euthanasia and enucleation ● Timing 10–15 min per mouse

▲ **CRITICAL** (Optional) A laser spot can be administered around the optic nerve on the opposite side of the injection site to enable beginners to better identify the injection site and keep it intact in the following procedures. Laser strength should be adjusted to enable creation of a small air bubble in the subretinal space for a choroidal neovascularization (CNV) induction. More details of the laser induction can be found in a published protocol

for CNV development in mice[56]. It is important to avoid laser impacts to the retinal vessels to prevent intraocular hemorrhage.

! CAUTION Use protective goggles to filter the wavelength of the laser to protect the eyes.

24 Euthanize mice following your approved protocol. We humanely euthanize the mice in a carbon dioxide chamber, using cervical dislocation as a secondary method of euthanasia.

25 Perform enucleation by inserting a curved Vannas scissor and cutting the four recti muscle at their insertion on the globe. Lift the eyeball, and cut the optic nerve. Collect the eye, and remove excess periocular muscles in PBS.

▲ **CRITICAL STEP** Careful manipulation of the eyeball is necessary during enucleation to prevent inadvertent opening up of the sclerotomy and collapse of the eyeball.

▲ **CRITICAL STEP** Perform Steps 25–26 on each mouse individually. Do not simultaneously euthanize and enucleate multiple mice.

(Optional) RPE and choroidal flat mounts ● Timing 3 h over 2 d

26 Fix the eye in 1 ml 2% PFA for 30 min at 4 °C.

27 Remove the anterior segment, lens, and retina, and apply four complete radial cuts in the RPE/choroid/sclera complex.

▲ **CRITICAL STEP** Radial cuts should be carefully placed to prevent injury to the injected area. Keeping the sclerotomy and the retinotomy on the same axis (Step 15) and laser-induced marker (Step 24) are two auxiliary ways to ensure the radical cuts are away from the injection area.

28 Wash with PBS three times, TBS three times and TBS-Triton-X (0.2%) three times.

29 Incubate RPE flat mounts with 400 μl of blocking buffer (0.75 g bovine serum albumin in 50 ml TBS-T) for 1 h in a rocker at 4 °C.

30 Incubate the RPE flat mounts overnight in a rocking platform at 4 °C with a primary antibody that targets the protein of interest such as Alexa Fluor 549-conjugated mouse ZO-1 (diluted 1:100 in blocking buffer).

31 Wash with TBS-T three times. If the primary antibody is conjugated (such as Alexa Fluor 549-conjugated mouse ZO-1), skip to Step 35.

32 Incubate the tissue section with appropriate secondary antibodies (such as goat anti-rabbit IgG (H+L), Alexa Fluor 594 conjugate if the primary antibody isotype is from rabbit) for 1 h. The conjugate of the secondary antibody can be chosen as needed.

33 Wash with TBS-T three times.

34 Wash with TBS five times, then mount the samples on glass slides with RPE layer face up using anti-fade mounting medium.

(Optional) Confocal imaging and image analysis ● Timing 6 h for 12 mice

35 Obtain images by confocal microscopy (model A1R Nikon confocal microscope system, Nikon). First identify the injection site and the surrounding area using lower magnification, then acquire images at higher magnification[15].

▲ **CRITICAL** The injection site is identified by the characteristic stellate pattern of the RPE at the injection site (Fig. 6)[15].

36 Quantify RPE degeneration based on ZO-1-stained flat mount images using semi-automated cellular morphometry analysis. For the results shown here, microscopy photos of the RPE were taken and transmitted in a deidentified fashion to the Doheny Image Reading & Research Lab (DIRRL). A step-by-step guide showing the analysis, illustrated by pictures, can be found in the Supplementary Manual.

Troubleshooting

Troubleshooting advice can be found in Table 2.

Timing

Steps 1–3, reagent and syringe preparation: 30 min for 12 mice

Steps 4–7, anesthesia and preparation of mice: 10 min per mouse

Steps 8–20, SRI injection: 1–1.5 h for 12 mice, depending on the combination of injection type

Step 21, mouse treatment: <3 min per mouse

Steps 22–23, fundus imaging: 30 min for 12 mice

Steps 24–25, mouse euthanasia and enucleation: 10–15 min per mouse

Steps 26–34 (Optional), RPE and choroidal flat mounts: 3 h over 2 d

Steps 35–36 (Optional), confocal imaging and image analysis: 6 h for 12 mice

Anticipated results

On the basis of previous work[7-16], we defined successful SRI both intraoperatively and post-operatively. For the postoperative definition of success, SRI of PBS results in no RPE degeneration after 7 d, as assessed by the absence of a sizeable hypopigmented area adjacent to the injection site in fundus imaging and normal cellular architecture of the RPE as visualized by confocal imaging of ZO-1-immunostained RPE flat mounts (Fig. 5a). Conversely, successful SRI of in vitro transcribed *Alu* RNA, which is cytotoxic to the RPE,

results in RPE degeneration evident after 7 days[7-14,16]. RPE degeneration is defined by the presence of a large hypopigmented area adjacent to the injection site in fundus imaging and by the disorganized and hypertrophic appearance of ZO-1-stained RPE flat mounts (Fig. 5b).

For beginners, high-resolution OCT scans performed immediately after injection can show the success of fluid delivery into the subretinal space. It can also help identify the changes of the outer retina and RPE (Fig. 7a-c, left column). Proper SRI of PBS should not cause RPE degenerative changes shown in OCT on both days 1 and 7 (Fig. 7a); however, a procedure that results in an expansive bleb after SRI can induce iatrogenic damage to the retina and the RPE, as evidenced by subretinal vacuolization in OCT on day 7 (Fig. 7b). Conversely, a proper bleb seen on OCT does not necessarily indicate a successful injection. For example, if the injection needle enters the subretinal space during the injection, the procedure itself could cause injection-related RPE damage even if the bleb flattens immediately after injection (Fig. 7c). Other relevant factors include injection speed and retinotomy force. The drawbacks of performing OCT immediately after injection include the additional movement of the mice, development of cataract in the contralateral eye and additional time consumption. A drawback of performing OCT in the follow-up period is extra anesthesia. We suggest OCT-guided examination during the training phase.

Another way of demonstrating the efficacy of this technique is to perform SRIs of 1 μl (10^{11} plaque-forming units (p.f.u.)/ml) of either an AAV encoding Cre recombinase driven by an RPE-specific promoter (AAV2-hRPE(0.8)-iCre-WPRE) or a control AAV (AAV2-CMV-Null)[57]. Successful AAV delivery and gene transduction is indicated by positive Cre expression in the RPE layer of AAV2-hRPE(0.8)-iCre-WPRE treated eyes (Fig. 5c) 10 d after injection and its absence in AAV2-CMV-Null treated eyes (Fig. 5d).

Extended Data

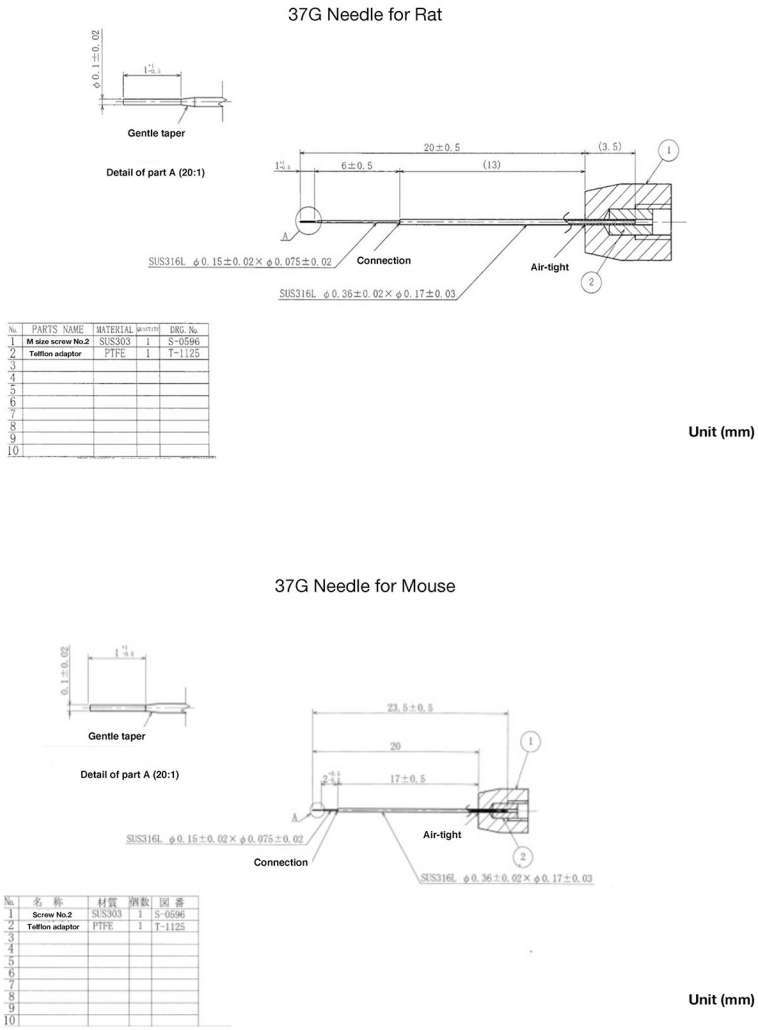

Extended Data Fig. 1 |. Custom needle parameters.

Detailed illustration of the needles designed for subretinal injection in rat (top) and mice (bottom).

Supplementary Material

Refer to Web version on PubMed Central for supplementary material.

Acknowledgements

J.A. has received support from the UVA Strategic Investment Fund, NIH grants (R01EY028027, R01EY29799 and R01EY31039), DuPont Guerry, III, Professorship, and a gift from Mr. and Mrs. Eli W. Tullis; B.D.G. has received support from NIH grants (R01EY028027, R01EY031039 and R01EY032512), BrightFocus Foundation and the Owens Family Foundation.

Data availability

All supporting data are available in the figures.

Related links

Key references using this protocol

References

Kaneko H. et al. Nature 471, 325–330 (2011): 10.1038/nature09830 [PubMed: 21297615]

Tarallo V. et al. Cell 149, 847–859 (2012): 10.1016/j.cell.2012.03.036 [PubMed: 22541070]

Kerur N. et al. Nat. Med 24, 50–61 (2018): 10.1038/nm.4450 [PubMed: 29176737]

References

1. Sharma S. et al. Pneumatic displacement of submacular hemorrhage with subretinal air and tissue plasminogen activator: initial United States experience. Ophthalmol. Retin 2, 180–186 (2018).
2. Herbert EN, Groenewald C & Wong D Treatment of retinal folds using a modified macula relocation technique with perfluoro-hexyloctane tamponade. Br. J. Ophthalmol 87, 921–922 (2003). [PubMed: 12812903]
3. Russell S. et al. Efficacy and safety of voretigene neparvovec (AAV2-hRPE65v2) in patients with RPE65-mediated inherited retinal dystrophy: a randomised, controlled, open-label, phase 3 trial. Lancet 390, 849–860 (2017). [PubMed: 28712537]
4. Pang JJ et al. Gene therapy restores vision-dependent behavior as well as retinal structure and function in a mouse model of RPE65 Leber congenital amaurosis. Mol. Ther 13, 565–572 (2006). [PubMed: 16223604]
5. Ling S. et al. Lentiviral delivery of co-packaged Cas9 mRNA and a Vegfa-targeting guide RNA prevents wet age-related macular degeneration in mice. Nat. Biomed. Eng 5, 144–156 (2021). [PubMed: 33398131]
6. Sun J. et al. Protective effects of human iPS-derived retinal pigmented epithelial cells in comparison with human mesenchymal stromal cells and human neural stem cells on the degenerating retina in rd1 mice. Stem Cells 33, 1543–1553 (2015). [PubMed: 25728228]
7. Kaneko H. et al. DICER1 deficit induces Alu RNA toxicity in age-related macular degeneration. Nature 471, 325–330 (2011). [PubMed: 21297615]
8. Tarallo V. et al. DICER1 loss and Alu RNA induce age-related macular degeneration via the NLRP3 inflammasome and MyD88. Cell 149, 847–859 (2012). [PubMed: 22541070]
9. Dridi S. et al. ERK1/2 activation is a therapeutic target in age-related macular degeneration. Proc. Natl Acad. Sci. USA 109, 13781–13786 (2012). [PubMed: 22869729]
10. Kerur N. et al. TLR-independent and P2X7-dependent signaling mediate Alu RNA-induced NLRP3 inflammasome activation in geographic atrophy. Invest. Ophthalmol. Vis. Sci 54, 7395–7401 (2013). [PubMed: 24114535]
11. Fowler BJ et al. Nucleoside reverse transcriptase inhibitors possess intrinsic anti-inflammatory activity. Science 346, 1000–1003 (2014). [PubMed: 25414314]
12. Kim Y. et al. DICER1/Alu RNA dysmetabolism induces Caspase-8-mediated cell death in age-related macular degeneration. Proc. Natl Acad. Sci. USA 111, 16082–16087 (2014). [PubMed: 25349431]
13. Gelfand BD et al. Iron toxicity in the retina requires Alu RNA and the NLRP3 inflammasome. Cell Rep. 11, 1686–1693 (2015). [PubMed: 26074074]
14. Kerur N. et al. cGAS drives noncanonical-inflammasome activation in age-related macular degeneration. Nat. Med 24, 50–61 (2018). [PubMed: 29176737]

15. Narendran S. et al. Nucleoside reverse transcriptase inhibitors and Kamuvudines inhibit amyloid-beta induced retinal pigmented epithelium degeneration. Signal Transduct. Target Ther 6, 149 (2021). [PubMed: 33850097]
16. Fukuda S. et al. Cytoplasmic synthesis of endogenous Alu complementary DNA via reverse transcription and implications in age-related macular degeneration. Proc. Natl Acad. Sci. USA 118, e2022751118 (2021). [PubMed: 33526699]
17. Fukuda S. et al. Alu complementary DNA is enriched in atrophic macular degeneration and triggers retinal pigmented epithelium toxicity via cytosolic innate immunity. Sci. Adv 7, eabj3658 (2011).
18. Little CW et al. Transplantation of human fetal retinal pigment epithelium rescues photoreceptor cells from degeneration in the Royal College of Surgeons rat retina. Invest. Ophthalmol. Vis. Sci 37, 204–211 (1996). [PubMed: 8550325]
19. Peng Y, Tang L & Zhou Y Subretinal injection: a review on the novel route of therapeutic delivery for vitreoretinal diseases. Ophthalmic Res. 58, 217–226 (2017). [PubMed: 28858866]
20. Iriyama A. et al. A2E, a component of lipofuscin, is pro-angiogenic in vivo. J. Cell Physiol 220, 469–475 (2009). [PubMed: 19418485]
21. Lyzogubov VV, Tytarenko RG, Liu J, Bora NS & Bora PS Polyethylene glycol (PEG)-induced mouse model of choroidal neovascularization. J. Biol. Chem 286, 16229–16237 (2011). [PubMed: 21454496]
22. Baba T. et al. A rat model for choroidal neovascularization using subretinal lipid hydroperoxide injection. Am. J. Pathol 176, 3085–3097 (2010). [PubMed: 20395434]
23. Narendran S. et al. A clinical metabolite of azidothymidine inhibits experimental choroidal neovascularization and retinal pigmented epithelium degeneration. Invest. Ophthalmol. Vis. Sci 61, 4 (2020).
24. Shen D, Wen R, Tuo J, Bojanowski CM & Chan CC Exacerbation of retinal degeneration and choroidal neovascularization induced by subretinal injection of Matrigel in CCL2/MCP-1-deficient mice. Ophthalmic Res. 38, 71–73 (2006). [PubMed: 16352919]
25. Jo YJ et al. Establishment of a new animal model of focal subretinal fibrosis that resembles disciform lesion in advanced age-related macular degeneration. Invest. Ophthalmol. Vis. Sci 52, 6089–6095 (2011). [PubMed: 21051730]
26. Georgiadis A. et al. Development of an optimized AAV2/5 gene therapy vector for Leber congenital amaurosis owing to defects in RPE65. Gene Ther. 23, 857–862 (2016). [PubMed: 27653967]
27. Xu H. et al. Subretinal delivery of AAV2-mediated human erythropoietin gene is protective and safe in experimental diabetic retinopathy. Invest. Ophthalmol. Vis. Sci 55, 1519–1530 (2014). [PubMed: 24508793]
28. Kim K. et al. Genome surgery using Cas9 ribonucleoproteins for the treatment of age-related macular degeneration. Genome Res. 27, 419–426 (2017). [PubMed: 28209587]
29. Holmgaard AB et al. Targeted knockout of the Vegfa gene in the retina by subretinal injection of RNP complexes containing Cas9 protein and modified sgRNAs. Mol. Ther 29, 191–207 (2021). [PubMed: 33022212]
30. Holmgaard A, Alsing S, Askou AL & Corydon TJ CRISPR gene therapy of the eye: targeted knockout of Vegfa in mouse retina by lentiviral delivery. Methods Mol. Biol 1961, 307–328 (2019). [PubMed: 30912054]
31. Wu L. et al. Subretinal gene delivery using helper-dependent adenoviral vectors. Cell Biosci. 1, 15 (2011). [PubMed: 21711866]
32. Huang R. et al. Functional and morphological analysis of the subretinal injection of human retinal progenitor cells under Cyclosporin A treatment. Mol. Vis 20, 1271–1280 (2014). [PubMed: 25352736]
33. McGill TJ et al. Subretinal transplantation of human central nervous system stem cells stimulates controlled proliferation of endogenous retinal pigment epithelium. Transl. Vis. Sci. Technol 8, 43 (2019).
34. Jin ZB et al. Stemming retinal regeneration with pluripotent stem cells. Prog. Retin. Eye Res 69, 38–56 (2019). [PubMed: 30419340]

35. Maya-Vetencourt JF et al. Subretinally injected semiconducting polymer nanoparticles rescue vision in a rat model of retinal dystrophy. Nat. Nanotechnol 15, 698–708 (2020). [PubMed: 32601447]
36. Fernandez-Bueno I, Alonso-Alonso ML, Garcia-Gutierrez MT & Diebold Y Reliability and reproducibility of a rodent model of choroidal neovascularization based on the subretinal injection of polyethylene glycol. Mol. Vis 25, 194–203 (2019). [PubMed: 30996588]
37. Lambert NG et al. Subretinal AAV2.COMP-Ang1 suppresses choroidal neovascularization and vascular endothelial growth factor in a murine model of age-related macular degeneration. Exp. Eye Res 145, 248–257 (2016). [PubMed: 26775053]
38. Luo L. et al. Photoreceptor avascular privilege is shielded by soluble VEGF receptor-1. eLife 2, e00324 (2013). [PubMed: 23795287]
39. Luo L. et al. Targeted intraceptor nanoparticle therapy reduces angiogenesis and fibrosis in primate and murine macular degeneration. ACS Nano 7, 3264–3275 (2013). [PubMed: 23464925]
40. Zhang X. et al. AAV2 delivery of Flt23k intraceptors inhibits murine choroidal neovascularization. Mol. Ther 23, 226–234 (2015). [PubMed: 25306972]
41. Cao J. et al. A subretinal matrigel rat choroidal neovascularization (CNV) model and inhibition of CNV and associated inflammation and fibrosis by VEGF trap. Invest. Ophthalmol. Vis. Sci 51, 6009–6017 (2010). [PubMed: 20538989]
42. Qiu G. et al. A new model of experimental subretinal neovascularization in the rabbit. Exp. Eye Res 83, 141–152 (2006). [PubMed: 16579984]
43. Timmers AM, Zhang H, Squitieri A & Gonzalez-Pola C Subretinal injections in rodent eyes: effects on electrophysiology and histology of rat retina. Mol. Vis 7, 131–137 (2001). [PubMed: 11435999]
44. Qi Y. et al. Trans-corneal subretinal injection in mice and its effect on the function and morphology of the retina. PLoS One 10, e0136523 (2015). [PubMed: 26317758]
45. Nickerson JM et al. Subretinal delivery and electroporation in pigmented and nonpigmented adult mouse eyes. Methods Mol. Biol 884, 53–69 (2012). [PubMed: 22688698]
46. Parikh S. et al. An alternative and validated injection method for accessing the subretinal space via a transcleral posterior approach. J. Vis. Exp 10.3791/54808 (2016).
47. Muhlfriedel R, Michalakis S, Garcia Garrido M, Biel M & Seeliger MW Optimized technique for subretinal injections in mice. Methods Mol. Biol 935, 343–349 (2013). [PubMed: 23150380]
48. Park SW, Kim JH, Park WJ & Kim JH Limbal approach-subretinal injection of viral vectors for gene therapy in mice retinal pigment epithelium. J. Vis. Exp 10.3791/53030 (2015).
49. Bennett J, Anand V, Acland GM & Maguire AM Cross-species comparison of in vivo reporter gene expression after recombinant adeno-associated virus-mediated retinal transduction. Methods Enzymol. 316, 777–789 (2000). [PubMed: 10800714]
50. Bartuma H. et al. In vivo imaging of subretinal bleb-induced outer retinal degeneration in the rabbit. Invest. Ophthalmol. Vis. Sci 56, 2423–2430 (2015). [PubMed: 25788649]
51. Matsumoto H, Miller JW & Vavvas DG Retinal detachment model in rodents by subretinal injection of sodium hyaluronate. J. Vis. Exp 10.3791/50660 (2013).
52. Huang P. et al. The learning curve of murine subretinal injection among clinically trained ophthalmic surgeons. Transl. Vis. Sci. Technol 10.1167/tvst.11.3.13 (2022).
53. de Melo J & Blackshaw S In vivo electroporation of developing mouse retina. Methods Mol. Biol 1715, 101–111 (2018). [PubMed: 29188509]
54. Zambricki EA & Dalecy LG Rat sex differences in anesthesia. Comp. Med 54, 49–53 (2004). [PubMed: 15027618]
55. Pritchett-Corning KR, Luo Y, Mulder GB & White WJ Principles of rodent surgery for the new surgeon. J. Vis. Exp 10.3791/2586 (2011).
56. Lambert V. et al. Laser-induced choroidal neovascularization model to study age-related macular degeneration in mice. Nat. Protoc 8, 2197–2211 (2013). [PubMed: 24136346]
57. Wright CB et al. Chronic Dicerl deficiency promotes atrophic and neovascular outer retinal pathologies in mice. Proc. Natl Acad. Sci. USA 117, 2579–2587 (2020). [PubMed: 31964819]

58. Wang S. et al. DDX is an essential mediator of sterile NLRC inflammasome activation. DDX17 is an essential mediator of sterile NLRC4 inflammasome activation by retrotransposon RNAs. Sci. Immunol (in press).

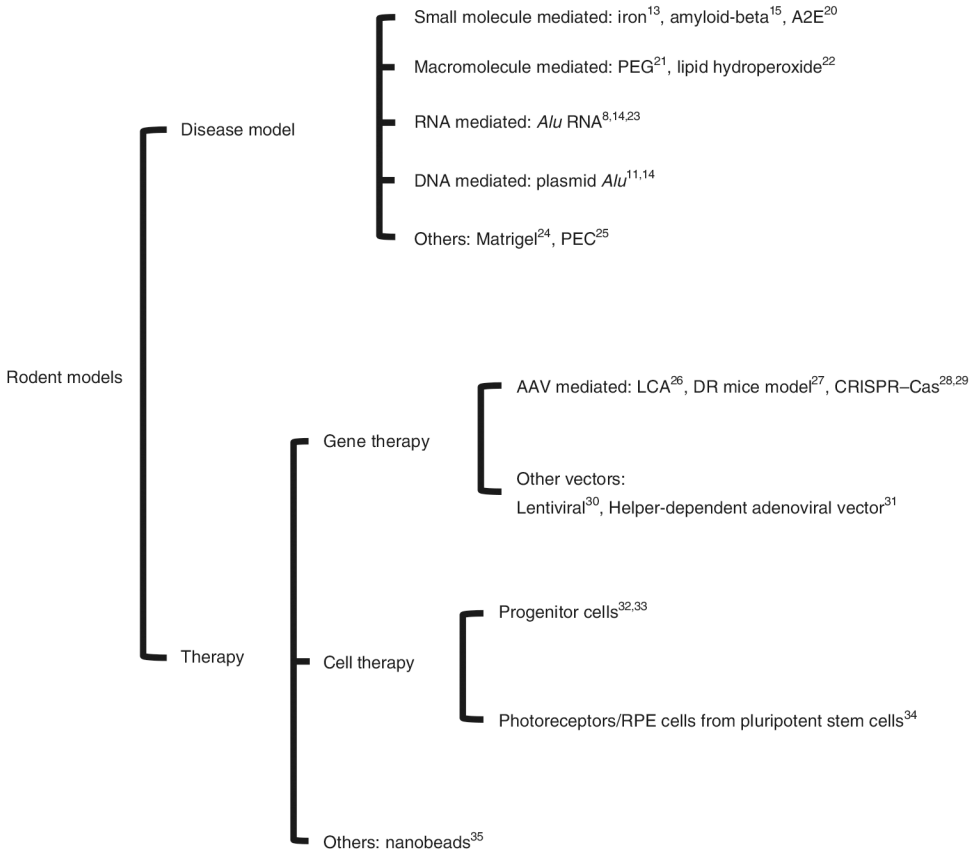

Fig. 1 |. Applications of SRI in rodent models.

SRI has been used in various applications, e.g., to deliver reagents to create disease models, for gene and cell replacement therapies. A2E, *N*-retinylidene-*N*-retinylethanolamine; DR, diabetic retinopathy; LCA, Leber Congenital Amaurosis; PEC, macrophage-rich peritoneal exudate cell.

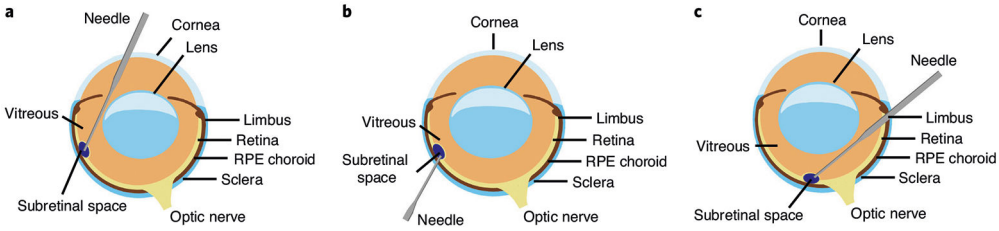

Fig. 2 |. Depictions of three SRI approaches.

a, The corneal approach. **b**, The transscleral posterior approach. **c**, The pars plana approach.

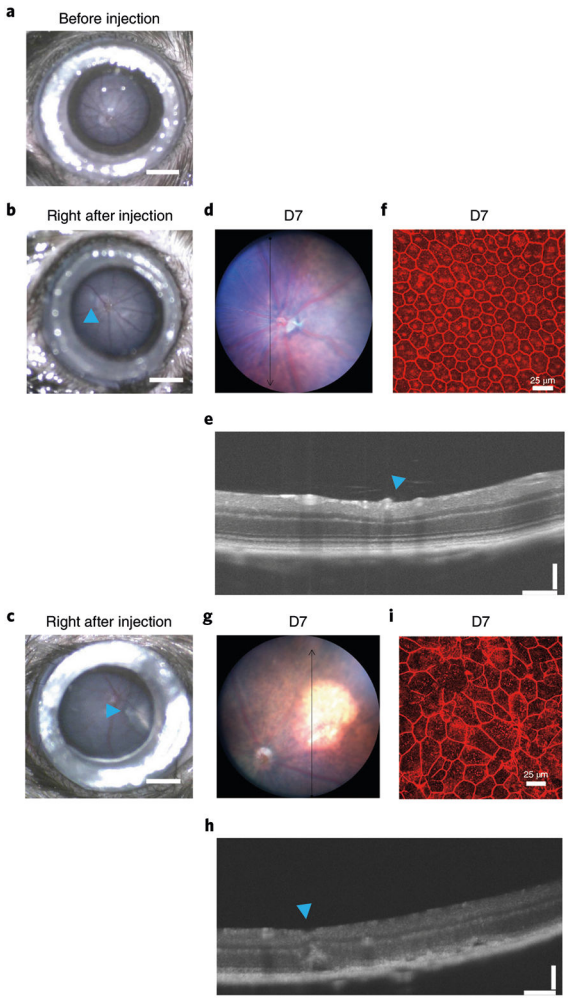

Fig. 3 | Representative images of a proper and improper SRI procedure to study the RPE phenotype.

a, Clear view of the fundus shown as seen through the surgical microscope after mounting the ocular ring on the eye and adding the lubricant gel. After adjusting the focus under the surgical microscope, we can clearly see the optic nerve located in the center of the field. Scale bar, 1 mm. **b**, Ideal postinjection fundus as visualized under the surgical microscope after SRI of 0.6 μl PBS. The blue triangle indicates the injection site. Scale bar, 1 mm. **c**, Extensive bleb (retinal detachment) as visualized under the surgical microscope induced by improper SRI of 0.6 μl PBS. Scale bar, 1 mm. **d**–**f**, The same eye as that observed in **b**; fundus photography (**d**) and OCT (**e**) showed no RPE degeneration (scale bar, 100 μm); confocal images of RPE flat mounts stained for ZO-1 also showed normal cellular architecture (scale bar, 25 μm) (**f**). **g**–**i**, The same eye as that observed in **c**; fundus photography (**g**) and OCT (**h**) showed hypopigmentation and subretinal vacuolization on day 7 (D7) (scale bar, 100 μm); confocal images of RPE flat mounts staining for ZO-1 showed disrupted cellular architecture (scale bar, 25 μm) (**i**).

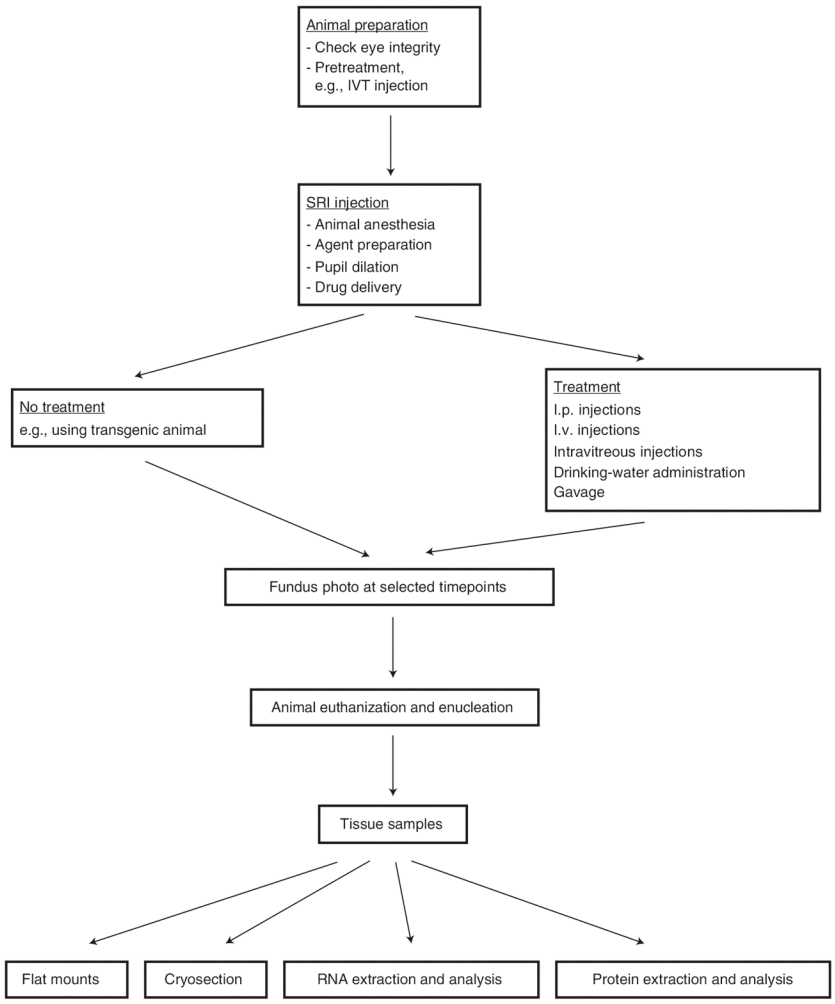

Fig. 4 |. Overview of the procedure.

The general protocol for SRI involves reagent and animal preparation (Steps 1–7) followed by SRI injection (Steps 8–20), additional experimental treatment (Step 21) or use of transgenic mice, fundus photo examination (Steps 22–23), euthanasia and enucleation (Steps 24–25), sample preparation (Steps 26–34) and confocal imaging (Steps 35–36). IVT, intravitreous; I.p., intraperitoneal; I.v., intravenous.

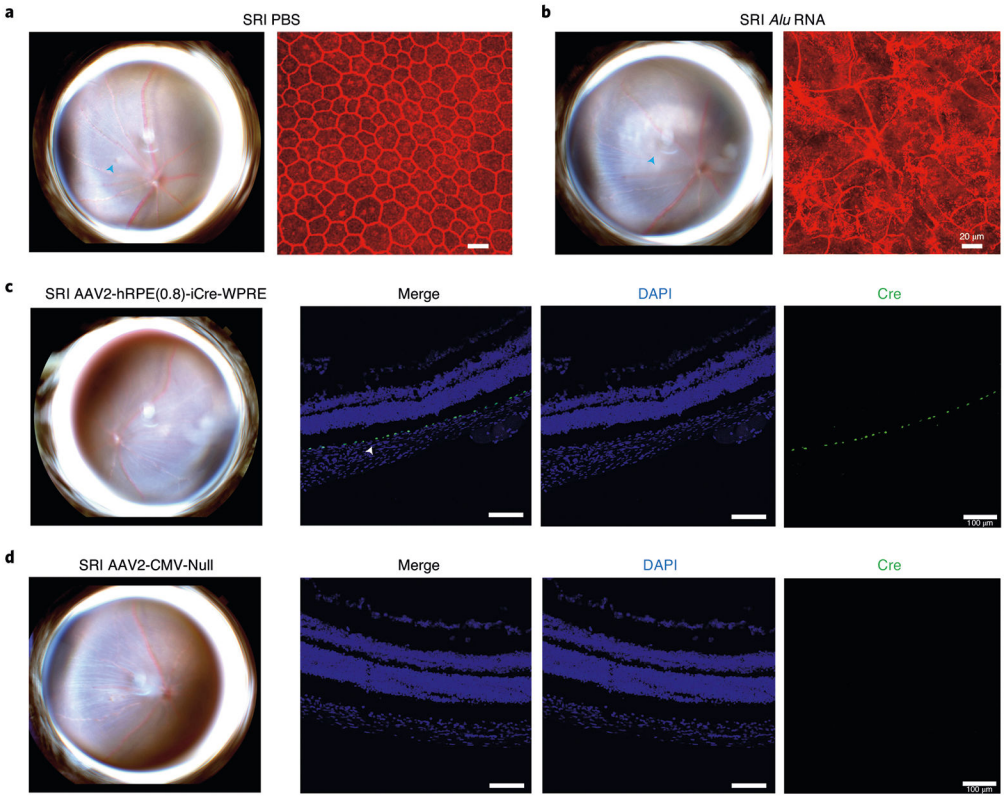

Fig. 5 | Representative images of a successful SRI.

a,**b**, Representative fundus photo (left) and flat mounts stained for ZO-1 (red, right). The pictures depict the classical phenotypic characteristics of mice administered with SRI of PBS (**a**, no degeneration) or *Alu* RNA (**b**, note focal hypopigmentation). Blue triangle, injection site. Scale bars, 20 μm. **c**,**d**, Representative fundus photo (left) and fluorescent micrographs of 10-μm-thick retinal sections labeled with DAPI and anti-Cre in C57BL/6J mice after injection of AAV2-hRPE(0.8)-iCre-WPRE (**c**) or AAV2-CMV-Null (**d**). Note the Cre expression 10 d after injection shown by white arrowheads (**c**). Scale bars, 100 μm. WPRE, woodchuck hepatitis posttranscriptional regulatory element.

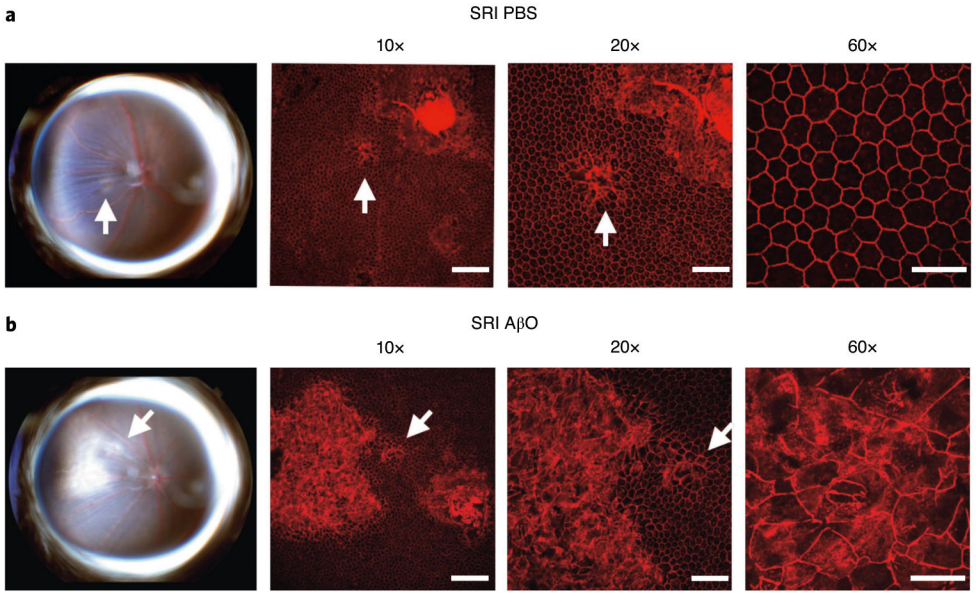

Fig. 6 | Identification of the injection site in mouse RPE flat mounts.

a,**b**, Fundus photographs (left) and RPE flat mounts stained for ZO-1 (red) at lower (10× and 20×) and higher magnifications (60×) after SRI of PBS (**a**) or AβOs (**b**). The injection site is identified by characteristic stellate pattern in the RPE (white arrow), which corresponds to the region where the needle touches the RPE. The surrounding area is examined, and higher-magnification images are acquired and analyzed. Scale bars, 10× (200 μm), 20× (100 μm) and 60× (50 μm). AβO, amyloid-beta oligomers. Figure reproduced with permission from ref. [15].

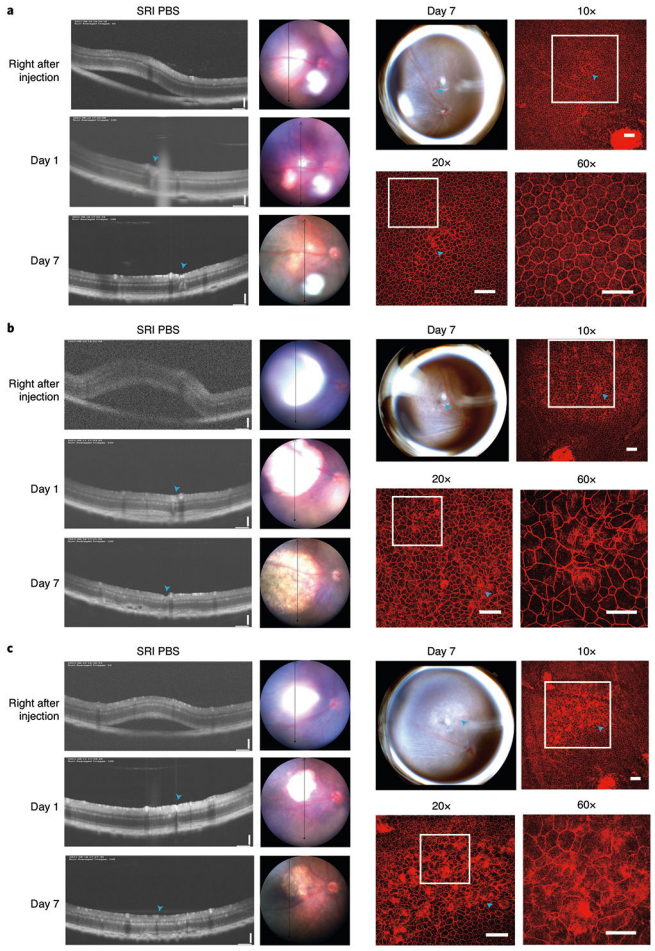

Fig. 7 |. Follow-up of successful and improper SRI of PBS.

a, After successful SRI of PBS, the retina reattaches as early as day 1 as visualized on OCT (left). On day 7, fundus photography showed no RPE degeneration, and OCT and confocal images of ZO-1-immunostained RPE flat mounts (red, right) at lower (10× and 20×) and higher magnification (60×) of the same eye showed normal RPE cellular architecture. **b**, After improper SRI, a bullous retinal detachment was observed intraoperatively. OCT showed RPE and outer retinal changes as early as day 1. On day 7, fundus photos showed areas of hypopigmentation, and OCT and confocal images of ZO-1-immunostained RPE flat mounts showed distorted RPE cellular architecture. **c**, An improper injection technique could also cause injection-related RPE degeneration, even flattening of the bleb. In this case, the injection needle has entered the subretinal space. Blue triangles indicate the site of the injection. Scale bars, 10× and 20× (100 μm), 60× (50 μm) for ZO-1 and 100 μm for OCT scans.

Table 1 |

Examples of positive and negative controls

	Suggested mass	Suggested volume	Suggested observation timepoints (d)	RPE degeneration observed (d)	Solute
Positive controls					
AAV1-BEST1-Cre in Dicer$^{f/f}$ mice[7]	10^{11}–10^{12} p.f.u./ml	0.3–1.0 μl	14	Start from day 10–14	10× PBS, ddH_2O
AAV2-hRPE(0.8)-iCre-WPRE in Dicer$^{f/f}$ mice[57]	10^{11}–10^{12} p.f.u./ml	0.3–1.0 μl	14	Start from day 10–14	10× PBS, ddH_2O
AβOs[15]	1 μM, 1 μl	0.5–1.0 μl	7	Start from day 5	10× PBS, ddH_2O
Alu RNA[8,23]	300 ng	0.5–1.0 μl	7	Start from day 5	10× PBS, ddH_2O
B2 RNA[58]	225 ng	0.5–1.0 μl	7	Start from day 5	10× PBS, ddH_2O
Cholesterol-conjugated B1/B2 antisense oligonucleotides[7]	2 μg	0.5–1.0 μl	7	Start from day 7	10× PBS, ddH_2O
Cholesterol-conjugated Dicer1 siRNA in vivo[14], Dicer1 siRNA: sense, CUCUGUGAGAGUUGUCCdTdT; control siRNA: sense, UAAGGCUAUGAAGAGAUdTdT)	1 μg	0.5–1.0 μl	7	Start from day 7	10× PBS, ddH_2O
Cr (VI)[13]	20 nM, 1 μl	0.5–1.0 μl	7	Start from day 5	10× PBS, ddH_2O
Cu (I)[13]	5 nM, 1 μl	0.5–1.0 μl	7	Start from day 5	10× PBS, ddH_2O
Fe (III)[13]	20 nM, 1 μl	0.5–1.0 μl	7	Start from day 5	10× PBS, ddH_2O
Plasmid expressing *Alu* sequences (p*Alu*)[11,14]	300 ng	0.5–1.0 μl	7	Start from day 7	10% Neoportor (Genlantis), OPTI, and 10× PBS mixture
Negative controls					
AAV1-BEST1-GFP[7]	10^{11}–10^{12} p.f.u./ml	0.3–1.0 μl	14	–	10× PBS, ddH_2O
AAV2-CMV-Null[57]	10^{11}–10^{12} p.f.u./ml	0.3–1.0 μl	14	–	10× PBS, ddH_2O
Empty-control vector (pNull)[11,14]	300 ng	0.5–1.0 μl	7	–	10% Neoportor (Genlantis), OPTI, and 10× PBS mixture
PBS;[7,8,13-15,23] refer to Step 1 for details	–	0.5–1.0 μl	7	–	10× PBS, ddH_2O

Table 2 |

Troubleshooting table

Step	Problem	Possible reason	Solution
6	Pupils are not dilated enough	Drop of tropicamide has dripped out	Place an additional drop of tropicamide on the eye, and ensure that the mouse does not remove it from the eye
7	Cataract development	Use of xylazine–ketamine mixture for anesthesia	Use Avertin as an anesthetic
	Death of mice	Anesthetic overdose Hypothermia	Single injection of Avertin should be sufficient Use temperature therapy pad
	Insufficient anesthesia	Incorrect dosage of anesthetic agent; lack of experience	Weigh the mice precisely Calculate the drug delivered accurately Avoid air bubbles when aspirating the anesthesia drug
13	Hydrogel slips from the ring circle	The concentration of the liquid gel is too low. We do not recommend standard artificial tears (0.25% of carboxymethylcellulose) The height and diameter of the ring does not match the cornea	1% carboxymethylcellulose sodium is recommended. Adjust the diameter of the ring to match the corneal diameter For 6- to 8-week-old mice, a ring of 3 mm diameter and 1.5 mm height is recommended
14	The optic nerve cannot be clearly seen	Mouse is incorrectly positioned Needle touches the lens and causes cataract	Adjust the position of the mouse on the head rest Avoid damaging the lens when advancing the needle To create the sclerotomy, do not introduce the full length of the 30 G needle
15	Bleeding from the sclerotomy	Rupture of the vasculature around the limbus	Avoid puncturing the blood vessel In most circumstances, the bleeding will stop by itself Gently wipe off the blood with a sterilized swab and continue the procedure if the bleeding is not intense (without blood flows into the eye cavity)
17	Subretinal space is not established	The reagent is delivered in the vitreous cavity or retina instead of the subretinal space	The angle between the needle and the retina should be 45° or less Optimize the microscope settings so that the wave of the reagent opening the subretinal space can be clearly seen Visualization of the RPE brownish pigmentation in the retinotomy site is a good sign there is full-thickness retinotomy
		The inner limiting membrane (ILM) or retina tissue obstructs the tip of the needle	Withdraw the tip a little bit to avoid/release the ILM or other retinal tissue in the needle lumen, and then advance the needle near to the retinotomy site again
		Liquid reflux	Visualization of a small fluid wave when injecting is a good sign of liquid delivery OCT examination after injection in the training periods
	Intraoperative subretinal/vitreous hemorrhage	Injury to retinal or choroidal blood vessel	It is essential to use a hand rest to support the surgeon's hand and the syringe to ensure stability during the injection Avoid touching the retinal vessel Avoid excessive pressure. Gentle pressure is sufficient to create a retinotomy If retinal bleeding is detected, exclude the eye from the analysis
19	Bullous retinal detachment is observed	The retinal detachment is too large, causing RPE degeneration	Avoid a large retinotomy by controlling hand stability Create an angulated retinotomy. The angle between the needle and the retina should be 45° or less Press the syringe plunger gently and slowly, giving time for the fluid to accommodate into the subretinal space Avoid intraocular pressure fluctuation during the procedure as intraoperative hypotony (large sclerotomy size or extensive manipulation) can increase the extent of retinal detachment
20	Postoperative infection	Contamination of the needle, syringe or reagents delivered	Sterilize the needle and syringe All the agents delivered should be prepared in a sterile environment PBS should be made fresh and used as a negative control to check any contamination
		Antibiotic ointment not used	Rapidly apply antibiotic ointment after the surgery
21	The solution is not injected into the vitreous	The solution enters the lens instead	The needle should enter into the eye at a 60° angle or more, and if the lens is damaged, the injection should be aborted

Step	Problem	Possible reason	Solution
	Wound leak from the sclerotomy	The needle has been taken out of the eye too early or too fast	Wait 20–30 s before taking the needle out of the eye
		The total volume of injection was too high	Do not inject more than 1 μl into the vitreous cavity